

Absorption and Fluorescence Signatures of 1,2,3-Triazole Based Regioisomers : Challenging Compounds for TD-DFT †

Claudine Katan^{*a}, Paul Savel^a, Bryan M. Wong^b, Thierry Roisnel^a,
Vincent Dorcet^a, Jean-Luc Fillaut^a, and Denis Jacquemin^{*c,d}

^a CNRS, Institut des Sciences Chimiques de Rennes, UMR6226-CNRS- Université de Rennes 1, 35042 Rennes Cedex, France. Tel: +33-2-23-23- 52-86. E-mail: claudine.katan@univ-rennes1.fr

^b Drexel University, Department of Chemistry, Department of Materials Science & Engineering, Philadelphia, PA 19104, USA

^c CEISAM, UMR CNRS 6230, BP 92208, Université de Nantes, 2, Rue de la Houssinière, 44322 Nantes, Cedex 3, France. Tel: +33-2-51-12-55-64

^d Institut Universitaire de France, 103 bd St Michel, 75005 Paris Cedex 5, France. E-mail: Denis.Jacquemin@univ-nantes.fr.

Synthesis.....	P2
Structural data.....	P3
Experimental absorption and emission spectra.....	P5
Calculated maximum of the first absorption band.....	P7
Comparison of calculated and experimental optical spectra	P8
Natural transition orbitals.....	P9
References.....	P9

Synthesis:

N,N-dimethyl-4-(1-phenyl-1H-1,2,3-triazol-4-yl)aniline (da) 4-iodobenzene (386 μ L, 3.45 mmol, 1.0 equiv.) was mixed with N,N-dimethyl-4-phenylacetylene (500 mg, 3.45 mmol, 1.0 equiv.) in a 20 mL scintillation vial. To the mixture were added L-proline (80 mg, 0.2 equiv.), Na₂CO₃ (150 mg, 0.4 equiv.), NaN₃ (269 mg, 1.2 equiv.), L-ascorbate acid (145 mg, 0.1 equiv.), 9:1 DMSO/H₂O (10 mL), and CuSO₄·5H₂O (43 mg, 0.05 equiv.). The mixture was stirred overnight at 65 °C. Upon completion (monitored by TLC), the crude mixture was poured into 30 mL of dilute NH₄OH solution and stirred during 30 min. The white precipitate was isolated by filtration and washed with dilute NH₄OH, water and then with cold methanol (ATTENTION: this step is important, as copper azides are explosive when dry, and their traces should be removed before the product is dried). The crude product was dissolved in CH₂Cl₂ and subjected to a chromatography on silica gel, with CH₂Cl₂ (to remove starting materials) followed by ethyl acetate as eluent. The product was obtained as a white powder (570 mg, 69%). ¹H NMR (400 MHz, CDCl₃) δ (ppm): 8.06 (s, 1H), 7.80 (m, 4H), 7.54 (m, 2H), 7.44 (t, J = 7.0 Hz, 1H), 6.80 (d, J = 8.2 Hz, 2H), 3.01 (s, 6H, Me). ¹³C NMR (100 MHz, CDCl₃) : δ 150.54, 148.93, 137.29, 129.70, 128.49, 126.86, 120.44, 118.47, 116.03, 112.59 , 40.50. Anal. found: C, 71.82; H, 5.81; N, 20.61. Calc. for C₁₆H₁₆N₄, 1/9 AcOEt: C, 71.96; H, 6.23; N, 20.36. m/z (Waters Q-TOF 2) 287.1269 (1 ppm) ; ([M+Na]⁺, C₁₆H₁₆N₄Na requires 287.12727).

N,N-dimethyl-4-(4-phenyl-1H-1,2,3-triazol-1-yl)aniline (dai) 4-ido-N,N-dimethylaniline (350 mg, 1.48 mmol, 1.0 equiv.) was mixed with phenylacetylene (220 μ L, 1.48 mmol, 1.0 equiv.) in a 20 mL scintillation vial. To the mixture were added L-proline (34 mg, 0.2 equiv.), Na₂CO₃ (65 mg, 0.4 equiv.), NaN₃ (115 mg, 1.2 equiv.), L-ascorbate acid (95 mg, 0.1 equiv.), 9:1 DMSO/H₂O (10 mL), and CuSO₄·5H₂O (19 mg, 0.05 equiv.). The mixture was stirred overnight at 65 °C. Upon completion (monitored by TLC), the crude mixture was poured into 30 mL of dilute NH₄OH solution and stirred during 30 min. The white precipitate was isolated by filtration and washed with dilute NH₄OH, water and then with cold methanol (ATTENTION: this step is important, as copper azides are explosive when dry, and their traces should be removed before the product is dried). The crude product was dissolved in CH₂Cl₂ and subjected to a chromatography on silica gel, with CH₂Cl₂ (remove starting materials), then ethyl acetate. The product was obtained as a white powder (191 mg, 72%). ¹H NMR (400 MHz, CDCl₃) δ (ppm): 8.07 (s, 1H), 7.91 (d, J = 7.2 Hz, 2H), 7.60 (d, J = 8.7 Hz, 2H), 7.43 (m, 2H), 7.35 (t, J = 6.8 Hz, 1H), 6.79 (d, J = 8.7 Hz, 2H), 3.03 (s, 6H, Me). ¹³C NMR (100 MHz, CDCl₃): δ (ppm): 150.57, 130.78, 128.86, 128.85, 128.65, 128.13, 126.95, 125.77, 121.93, 112.42, 40.48. Anal. found: C, 72.56; H, 5.89; N, 20.70. C₁₆H₁₆N₄ Calc.: C, 72.70; H, 6.10; N, 21.20. m/z (Waters Q-TOF 2) 287.1268 (2 ppm) ; ([M+Na]⁺, C₁₆H₁₆N₄Na requires 287.12727). m/z 265.1453 (0 ppm) ; ([M+H]⁺, C₁₆H₁₇N₄ requires 265.14532).

Structural data: (full structural reports are provided as separate files).

Table S1. Bond lengths and inter-ring dihedral angles of **da**. Labels are given Figure S1. All calculated data use the 6-31+G(d) atomic basis set except HF geometries for which the 6-31G atomic basis set was used.ⁱ Distances are given in Å and angles in degrees. GS and ES label ground and excited state optimized geometries, respectively. Medium is given in parentheses (gas=gas phase, tol=toluene and THF=tetrahydrofuran).

Atom1	Atom2	X-Ray		GS	GS	GS	GS	ES	$\Delta(GS-ES)$
		mol. N°	mol. N°	HF (gas)	_PBE (tol)	CAM (tol)	ω B97X (THF)	ω B97X-D (THF)	Δ (GS-ES) (THF)
C1	C2	1.386(3)	1.391(3)	1.385	1.391	1.39	1.392	1.392	1.386 0.006
C1	C6	1.386(2)	1.392(2)	1.388	1.395	1.392	1.393	1.393	1.414 -0.021
C2	C3	1.387(3)	1.387(2)	1.388	1.395	1.393	1.394	1.395	1.401 -0.006
C3	C4	1.382(3)	1.382(3)	1.387	1.394	1.392	1.394	1.394	1.398 -0.004
C4	C5	1.388(3)	1.392(3)	1.387	1.392	1.391	1.393	1.393	1.388 0.005
C5	C6	1.387(2)	1.381(2)	1.387	1.395	1.392	1.392	1.393	1.413 -0.020
C6	N7	1.433(2)	1.436(2)	1.416	1.417	1.423	1.427	1.424	1.379 0.045
N7	N8	1.357(2)	1.357(2)	1.346	1.343	1.342	1.337	1.342	1.412 -0.070
N7	C11	1.358(2)	1.355(2)	1.359	1.356	1.356	1.355	1.355	1.367 -0.012
N8	N9	1.321(2)	1.317(2)	1.281	1.295	1.296	1.297	1.299	1.277 0.022
N9	C10	1.372(2)	1.368(2)	1.373	1.367	1.366	1.365	1.366	1.373 -0.007
C10	C11	1.375(3)	1.383(2)	1.366	1.381	1.377	1.377	1.379	1.420 -0.041
C10	C12	1.466(3)	1.469(2)	1.462	1.461	1.467	1.471	1.467	1.409 0.058
C12	C13	1.395(2)	1.397(3)	1.393	1.400	1.397	1.398	1.399	1.427 -0.028
C12	C17	1.394(2)	1.395(2)	1.391	1.400	1.397	1.398	1.399	1.436 -0.037
C13	C14	1.387(3)	1.389(3)	1.381	1.387	1.386	1.388	1.388	1.364 0.024
C14	C15	1.404(2)	1.404(2)	1.403	1.413	1.410	1.412	1.413	1.442 -0.029
C15	C16	1.407(3)	1.413(2)	1.403	1.413	1.410	1.411	1.412	1.422 -0.010
C15	N18	1.385(2)	1.384(2)	1.384	1.378	1.384	1.385	1.382	1.356 0.026
C16	C17	1.386(3)	1.386(3)	1.382	1.387	1.387	1.389	1.388	1.378 0.010
N18	C19	1.442(3)	1.449(3)	1.452	1.446	1.450	1.452	1.451	1.457 -0.006
N18	C20	1.434(2)	1.435(3)	1.451	1.445	1.450	1.452	1.451	1.454 -0.003
dihedral angle	ring1ring2	X-Ray		GS	GS	GS	GS	GS	$\Delta(GS-ES)$
		mol. N°	mol. N°	HF (gas)	_PBE (tol)	CAM (tol)	ω B97X (THF)	ω B97X-D (THF)	ω B97X-D (THF)
C1C6N7N8	AB	-17.8(2)	21.0(2)	-30.9	-29.0	-32.8	-35.9	-36.5	-4.1 -32.4
C5C6N7C11	AB	-17.7(3)	19.9(3)	-31.4	-29.3	-32.9	-36.2	-36.8	-2.9 -33.9
N9C10C12C13	BC	15.8(3)	24.8(2)	1.8	8.4	8.4	13.9	15.8	0.6 15.2
C11C10C12C17	BC	17.2(3)	22.9(3)	2.4	9.3	9.2	14.8	16.6	0.4 16.2

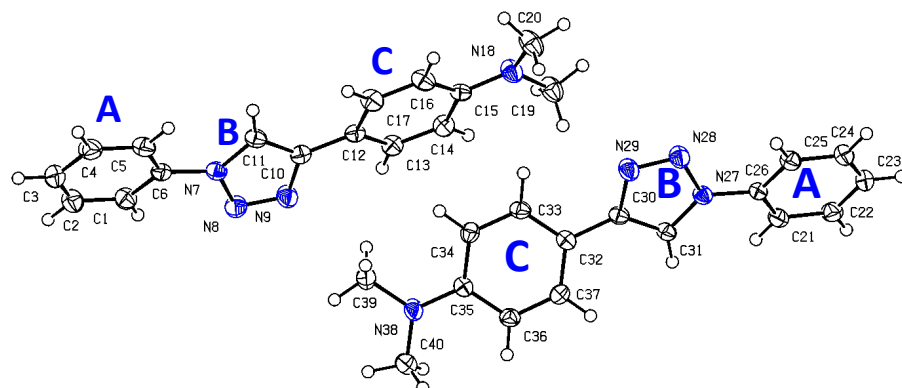


Figure S1. ORTEP representation of **da** molecules : N° 1 (top) and 2 (bottom), with atomic and ring labels.

Table S2. Bond lengths and inter-ring dihedral angles of **dai**. Labels are given Figure S2. All calculated data use the 6-31+G(d) atomic basis set except HF geometries for which the 6-31G atomic basis set was used.ⁱⁱ Distances are given in Å and angles in degrees. GS and ES label ground and excited state optimized geometries, respectively. Medium is given in parentheses (gas=gas phase, tol=toluene and THF=tetrahydrofuran).

Atom1	Atom2	X-Ray	GS	GS	GS	GS	GS	ES	$\Delta(GS-ES)$
		HF (gas)	PBE (tol)	CAM (tol)	ω B97X (THF)	ω B97X-D (THF)	ω B97X-D (THF)	ω B97X-D (THF)	$\Delta(GS-ES)$
C1	C2	1.388(2)	1.386	1.392	1.39	1.392	1.392	1.39	0.002
C1	C6	1.395(2)	1.394	1.401	1.398	1.399	1.400	1.405	-0.005
C2	C3	1.393(2)	1.388	1.395	1.393	1.394	1.395	1.398	-0.003
C3	C4	1.385(2)	1.387	1.395	1.393	1.394	1.394	1.394	0.000
C4	C5	1.385(2)	1.386	1.392	1.39	1.392	1.392	1.392	0.000
C5	C6	1.396(2)	1.394	1.401	1.399	1.399	1.400	1.405	-0.005
C6	C7	1.472(2)	1.465	1.465	1.470	1.474	1.471	1.460	0.011
C7	C11	1.374(2)	1.368	1.382	1.378	1.378	1.380	1.390	-0.010
C7	N8	1.368(2)	1.370	1.363	1.363	1.363	1.363	1.361	0.002
C11	N10	1.351(2)	1.354	1.352	1.352	1.352	1.352	1.390	-0.038
N9	N10	1.354(1)	1.346	1.343	1.343	1.337	1.342	1.420	-0.078
N10	C12	1.430(2)	1.419	1.418	1.424	1.428	1.425	1.343	0.082
N8	N9	1.314(2)	1.283	1.297	1.297	1.298	1.301	1.303	-0.002
C12	C13	1.389(2)	1.384	1.393	1.390	1.391	1.391	1.438	-0.047
C12	C17	1.383(2)	1.386	1.393	1.390	1.391	1.392	1.440	-0.048
C13	C14	1.383(2)	1.838	1.388	1.387	1.388	1.388	1.367	0.021
C14	C15	1.406(2)	1.403	1.413	1.411	1.413	1.414	1.434	-0.020
C15	C16	1.406(2)	1.405	1.414	1.412	1.413	1.415	1.434	-0.019
C15	N18	1.386(2)	1.382	1.375	1.379	1.379	1.377	1.359	0.018
C16	C17	1.384(2)	1.381	1.386	1.386	1.387	1.387	1.365	0.022
N18	C19	1.440(2)	1.452	1.445	1.45	1.452	1.451	1.454	-0.003
N18	C20	1.449(2)	1.453	1.446	1.45	1.452	1.452	1.454	-0.002
dihedral angle		X-Ray	GS	GS	GS	GS	GS	ES	$\Delta(GS-ES)$
ring1ring2		HF (gas)	PBE (tol)	CAM (tol)	ω B97X (THF)	ω B97X-D (THF)	ω B97X-D (THF)	ω B97X-D (THF)	$\Delta(GS-ES)$
C1C6C7N8	AB	-19.2(2)	1.3	0.3	0.5	11.8	13.3	0.0	13.3
C5C6C7C11	AB	-18.3(2)	1.9	0.9	1.0	12.4	14.0	0.0	14.0
C11N10C12C13	BC	-29.5(2)	-41.7	-36.4	-40.4	-43.9	-44.6	0.0	-44.6
N9N10C12C17	BC	-26.9(2)	-42.2	-37.1	-41.0	-44.5	-45.0	0.0	-45.0

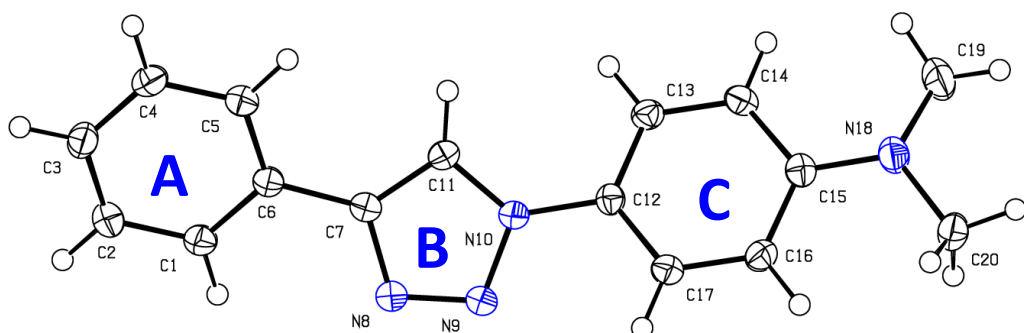


Figure S2. ORTEP representation of **dai** with atomic and ring labels.

Experimental absorption and emission spectra:

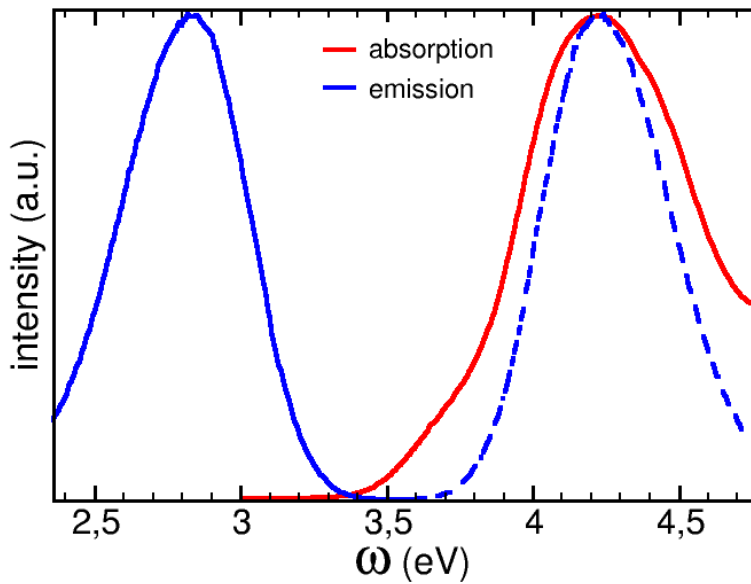


Figure S3. Normalised fluorescence (blue) and absorption (red) spectra of **da**. The dashed blue line is obtained by mirroring the fluorescence spectra so as to reveal non-mirror shapes of absorption and fluorescence spectra.

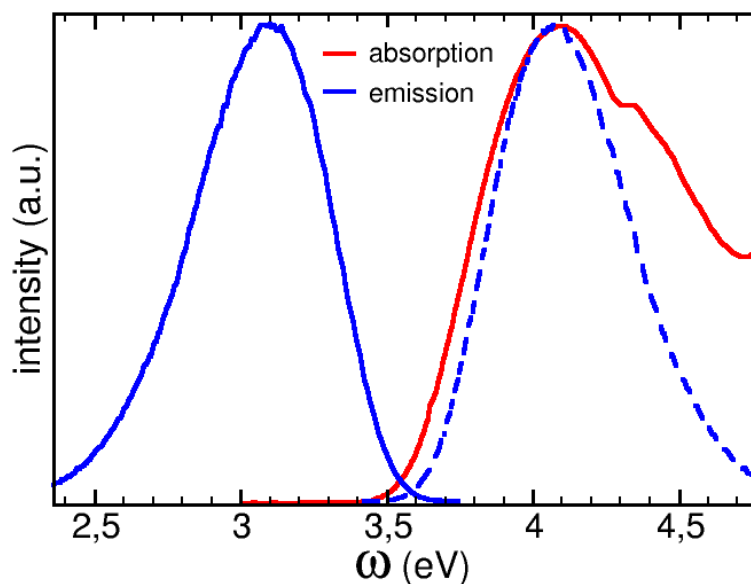


Figure S4. Normalised fluorescence (blue) and absorption (red) spectra of **dai**. The dashed blue line is obtained by mirroring the fluorescence spectra so as to reveal almost mirror shapes of absorption and fluorescence spectra.

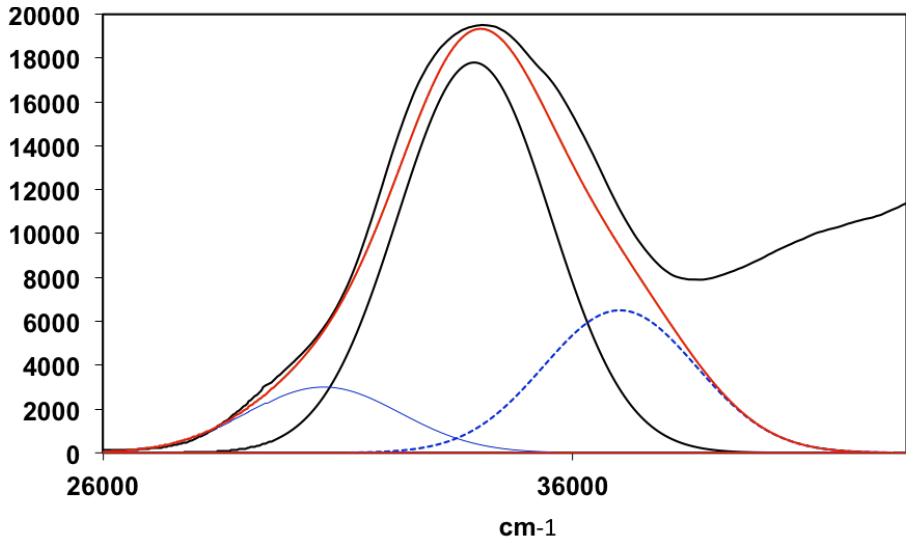


Figure S5. Tentative deconvolution of the experimental absorption spectrum of **da** recorded in THF (black line) using three Gaussian functions: $A_i \exp[-(\omega - \omega_i)^2 / (\alpha^2)]$. Widths are kept constant ($\alpha = 2300 \text{ cm}^{-1}$, *i.e.* FWHM of 0.47 eV), amplitudes and position are $A_1 = 3000$, $\omega_1 = 30700 \text{ cm}^{-1}$; $A_2 = 17800$, $\omega_2 = 33900 \text{ cm}^{-1}$; $A_3 = 6500$, $\omega_3 = 37000 \text{ cm}^{-1}$.

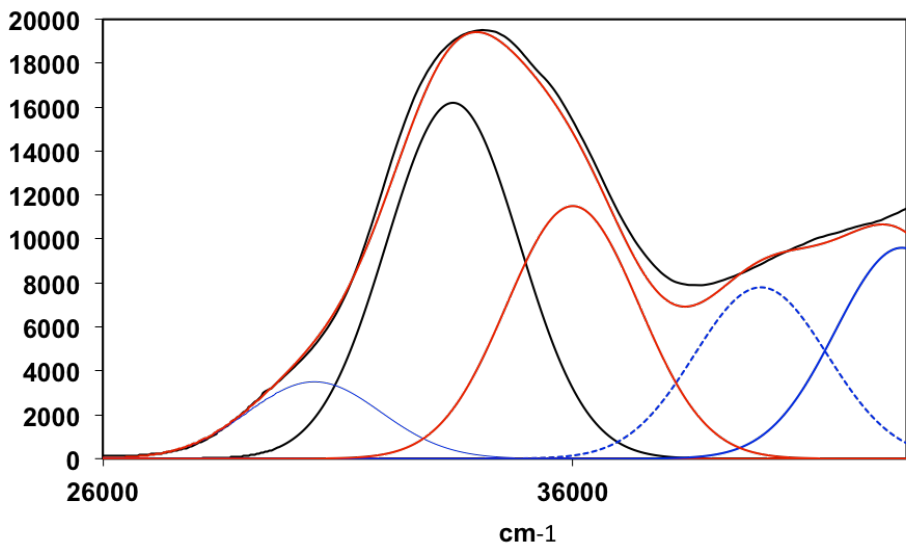


Figure S6. Tentative deconvolution of the experimental absorption spectrum of **da** recorded in THF (black line) using five Gaussian functions: $A_i \exp[-(\omega - \omega_i)^2 / (\alpha^2)]$. Widths are kept constant ($\alpha = 2000 \text{ cm}^{-1}$, *i.e.* FWHM of 0.41 eV), amplitudes and position are $A_1 = 3500$, $\omega_1 = 30500 \text{ cm}^{-1}$; $A_2 = 16200$, $\omega_2 = 33450 \text{ cm}^{-1}$; $A_3 = 11500$, $\omega_3 = 36000 \text{ cm}^{-1}$; $A_4 = 7800$, $\omega_4 = 40000 \text{ cm}^{-1}$; $A_5 = 9600$, $\omega_5 = 43000 \text{ cm}^{-1}$.

Comparison of Figure S3 with Figure S4 clearly reveals the non-mirror shape of the absorption spectrum of **da**. Tentative deconvolutions of the experimental absorption spectrum of **da** in THF using Gaussian functions are shown Figure S5 and S6. They lead of a splitting between the first two excited states of *ca* 0.4 eV. We underline that such a fitting procedure is relatively arbitrary and does not account for the asymmetric band shape provided by vibronic contributions. This leads us to report intervals (e.g. [0.3-0.5]) instead of a single value.

Calculated maximum of the first absorption band:

Table S3. Position of the maximum of the first absorption band (ω_{\max}^{abs}) obtained after convolution of the ES data given in Table 4 and considering two Gaussians having a FWHM of 0.50 eV. Values have been calculated in gas phase and are reported in eV.

Method	da	dai
EOM-CCSD/6-31G(d) ^a	5.03	5.22
RI-CC2/SVP ^b	4.66	4.93
LC-BLYP/SVP ^b	4.78	5.01
ω B97X-D/SVP ^b	4.72	4.96
ω B97X-D/6-31G(d) ^b	4.76	5.00
ω B97X-D/6-31G(d) ^b	4.65	4.87
ω B97X-D/6-31+G(d) ^c	4.64	4.81
CAM-B3LYP/6-31+G(d) ^a	4.53	4.71
B3LYP/SVP ^b	4.61	4.30
PBE0/6-31+G(d) ^a	4.57	4.31

^aCAM-B3LYP geometry

^bHF geometry

^c ω B97X-D geometry

Table S4. Position of the maximum of the first absorption band (ω_{\max}^{abs}) obtained after convolution of the ES data given in Table 5 and considering two Gaussians having a FWHM of 0.50 eV. Values have been calculated using the continuum PCM model in its non-equilibrium limits and are reported in eV.

Functional (medium)	PCM Model	da	dai
PBE0 (toluene)	LR	3.66	4.11
	cLR	3.36	4.01
	SS	2.43	2.72
PBE0 (THF)	LR	4.29	4.07
	cLR	4.19	3.91
	SS	2.59	2.64
CAM-B3LYP (Toluene)	LR	4.48	4.65
	cLR	4.51	4.67
	SS	4.58	4.47
CAM-B3LYP (THF)	LR	4.52	4.65
	cLR	4.55	4.65
	SS	4.52	4.35
CAM-B3LYP (DCM)	LR	4.52	4.64
	cLR	4.56	4.65
	SS	4.53	4.33
ω B97X (THF)	LR	4.76	4.93
	cLR	4.82	4.98
	SS	4.77	4.85
ω B97X-D (THF)	LR	4.61	4.67
	cLR	4.65	4.76
	SS	4.59	4.52

Comparison between theoretical and experimental optical spectra:

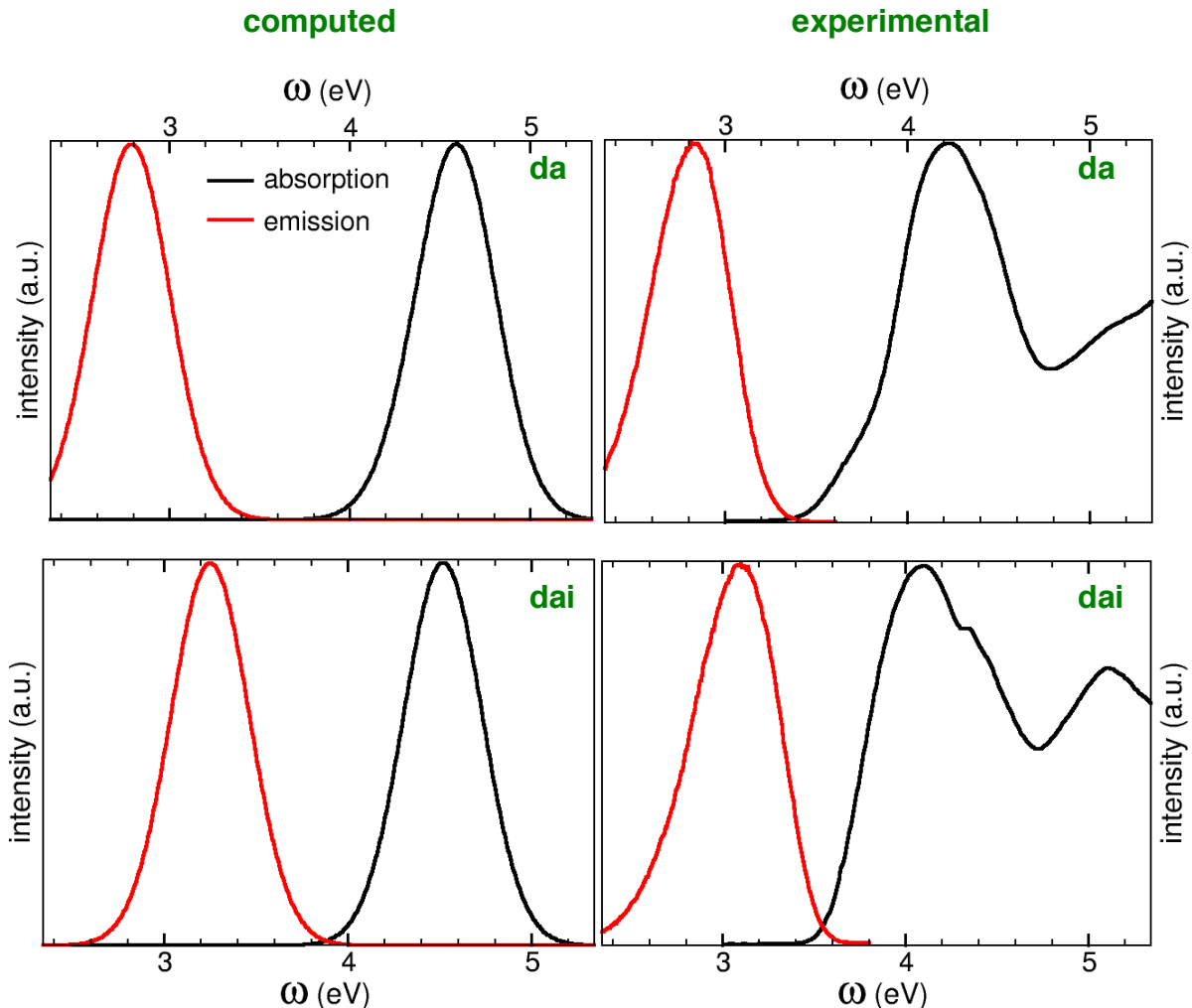
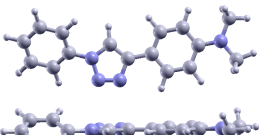
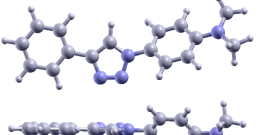
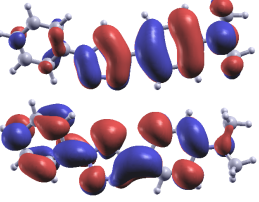
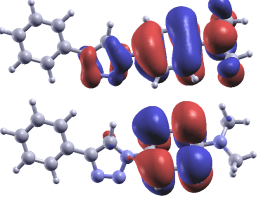
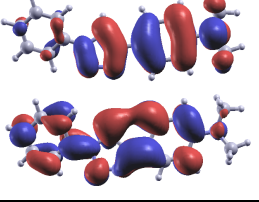
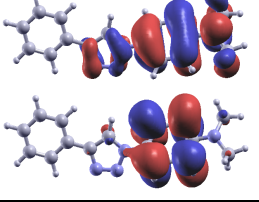
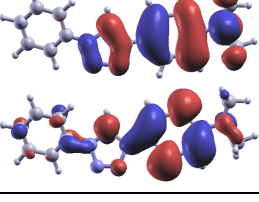
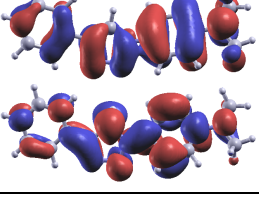
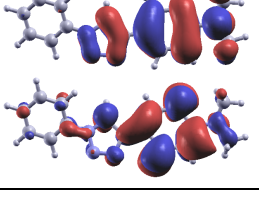
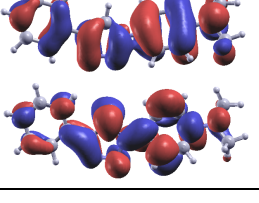


Figure S7. Computed (left) and experimental (right) emission (red) and absorption (black) spectra of **da** (top) and **dai** (bottom) in THF. Simulated spectra have been obtained taking transition energies and oscillator strengths from Table 6 and 7 for the ω B97X-D functional and SS approach for the PCM model. Band shapes have been obtained using Gaussians having a FWHM of 0.50 eV. We underline that Gaussians do not introduce band asymmetry in the band-shapes; simulating such asymmetry needs to compute vibrationally resolved optical spectra that are not yet available within the PCM-SS model. Calculated absorption spectra are based on the first two excited states and do not include states relevant for the increase in absorption experimentally observed at higher energies.

Table S5. Natural transition orbitalsⁱⁱⁱ of **da** (left) and **dai** (right) illustrating the effect of basis set for calculation in gas phase using geometries optimized at the CAM-B3LYP/6-31+G(d) level. Panels quote excited state number, associated eigenvalue, transition energy, transition wavelength and oscillator strength. Geometries and orbitals were plotted using XCrySDen.^{iv}

level of theory		da		dai
geometry: CAM-B3LYP/6-31+G(d)				
level of theory		hole electron		hole electron
TD-CAM-B3LYP/6-31G(d)	<1 w=0.94 4.58 eV 271 nm f ₀₁ =0.52		<1 w=0.89 4.78 eV 259 nm f ₀₁ =0.05	
TD-CAM-B3LYP/6-31+G(d)	<1 w=0.95 4.35 eV 285 nm f ₀₁ =0.38		<1 w=0.91 4.61 eV 269 nm f ₀₁ =0.07	
TD-CAM-B3LYP/6-31G(d)	<2 w=0.88 4.84 eV 256 nm f ₀₂ =0.36		<2 w=0.90 4.90 eV 253 nm f ₀₂ =1.00	
TD-CAM-B3LYP/6-31+G(d)	<2 w=0.90 4.68 eV 265 nm f ₀₂ =0.41		<2 w=0.89 4.72 eV 263 nm f ₀₂ =0.85	

ⁱ C. Katan, M. Blanchard-Desce and S. Tretiak, *Position Isomerism on One and Two Photon Absorption in Multibranched Chromophores: A TDDFT Investigation*, J. Chem. Theory Comput., 2010, **6**, 3410–3426 S.. J. Chem. Theory Comput. 2010, **6** , 3410-3426.

ⁱⁱ C. Katan, S. Tretiak and J. Even, *Two-photon transitions in triazole based quadrupolar and octupolar chromophores: a TD-DFT investigation*, Proc. SPIE, Int. Soc. , 2010, **7712**, 77123D.

ⁱⁱⁱ R. L. Martin, *J. Chem. Phys.* **2003**, *118*, 4775-4777.

^{iv} A. Kokalj, *Comp. Mater. Sci.* **2003**, *28*, 155-168. . Code available from <http://www.xcrysden.org/>.